

# Excitation of Surface Plasmons in Subwavelength Nanoapertures with Different Geometries

Feng Gao, Jinzhu Zhao, Dongxiang Qi, Qing Hu, Ruili Zhang, and Ruwen Peng\*

National Laboratory of Solid State Microstructures and Department of Physics, Nanjing University, Nanjing 210093, China

In this work, we investigate the transmission of light through an isolated subwavelength hole, the hole chain and the hole array with different geometries, respectively. It is shown that when the light illuminates an isolated subwavelength hole, localized surface plasmons (LSPs) are excited and contribute to transmission of the hole; while the light illuminates the hole chain and array, both LSPs and propagating surface plasmons (PSPs) are excited, and their contributions to the transmission of holes strongly depend on the geometry of the hole chain and array, and also on the polarization of incident light. The theoretical calculations are based on three-dimensional full-vector finite-difference time-domain method. The investigations may have potential applications on designing plasmonic structures and devices.

**Keywords:** Plasmonics, Subwavelength Optics, Nanoapertures.

## 1. INTRODUCTION

Since Ebbesen et al.<sup>1</sup> reported the extraordinary optical transmission (EOT) through a two-dimensional array of subwavelength holes perforated on silver film in 1998, much attention has been paid to the propagation of light through subwavelength apertures.<sup>2–10</sup> The results of EOT have challenged Bethe's predictions in 1944.<sup>11</sup> According to Bethe's theory, transmission intensity through an individual subwavelength aperture satisfied  $(r/\lambda)^4$ , where  $r$  is the hole radius and  $\lambda$  is the wavelength of incident light. We would expect that the optical transmission may drop rapidly as  $\lambda$  becomes larger than  $r$ . However in the EOT experiments, the optical transmission remains strong even if  $\lambda$  is much larger than the hole radius, and the zero-order transmission spectra exhibit well-defined maxima. It is generally accepted that the EOT originates from the interaction of surface plasmon polariton (SPP), a collective excitation of free electrons in metal film, with the lattice structure on metal film.<sup>1–5</sup> The SPP enhances the evanescent field at the apertures and thus contributes to funnel light through the hole array.<sup>5,6</sup> The SPP-based circuits can combine photonics and electronics on nano-scale, which offers the potential applications in plasmonic chips, nanolithography, and biophotonics.<sup>12</sup> However, it is interesting to identify how localized surface plasmons<sup>10</sup> (LSPs) and propagating surface plasmons<sup>6</sup> (PSPs) are excited and how they affect the transmission of nanoapertures.

In this work, based on three-dimensional full-vector finite-difference time-domain (FDTD) method, we theoretically investigate the transmission of light through an isolated subwavelength hole, the hole chain and the hole array with different geometries, respectively. It is shown that when the light illuminates an isolated subwavelength hole, LSPs are excited and contribute to transmission of the hole; while the light illuminates the hole chain and array, both LSPs and PSPs are excited, and their contributions to the transmission of holes strongly depend on the geometry of the hole chain and array, and also on the polarization of incident light.

## 2. THE THEORETICAL ANALYSIS

It is known that the enhancement of transmission is due to light coupling with SPs in the metallic-dielectric surface. In the metal film with a periodic array of holes, the interaction between light and the SP obeys momentum conservation,

$$\vec{k}_{sp} = \vec{k}_0 \sin \theta + (i\vec{G}_x + j\vec{G}_y) \quad (1)$$

where  $\vec{k}_{sp}$  is the wave vector of the SP,  $\vec{k} \sin \theta$  is the in-plane component of the incident wave vector,  $\vec{G}_x$  and  $\vec{G}_y$  are the reciprocal lattice vectors with the same value as  $|\vec{G}_x| = |\vec{G}_y| = 2\pi/a_0$ , and  $i, j$  are both integers. On the other hand, there exists the coupling of SPs in the structured metal/dielectric system.<sup>3</sup> In order to describe the dispersion relation of SPs in these systems, we use an effective permittivity  $\epsilon_{eff}$  of the structured metal instead of the previous

\*Author to whom correspondence should be addressed.

permittivity  $\epsilon_m$  of the metal. Here we assume that the light through the structured metal film can be effectively considered as that through an uniform metal with  $\epsilon_{\text{eff}}$ , and both cases have identical optical transmission and reflection on the planar film. Thereafter, the SP dispersion relation at the metal-dielectric interface can be rewritten as:

$$k_{\text{sp}} = k_0 \sqrt{\frac{\epsilon_d \cdot \epsilon_{\text{eff}}}{\epsilon_d + \epsilon_{\text{eff}}}} \quad (2)$$

Considering Eqs. (1) and (2) in the case of normal incidence  $\theta = 0$ , we can obtain the maxima transmission satisfying

$$\lambda_{\text{max}} = \frac{a_0}{\sqrt{i^2 + j^2}} \sqrt{\frac{\epsilon_d \cdot \epsilon_{\text{eff}}}{\epsilon_d + \epsilon_{\text{eff}}}} \quad (3)$$

Therefore, the transmission peaks can be indexed with integers  $(i, j)$  in the optical spectra. The effective permittivity of the structured metal  $\epsilon_{\text{eff}}$  can be derived from the reflectivity and transmittivity of light in the metal-dielectric system.

Another interesting characteristic of the transmission spectra is the transmission minima. The minima was usually identified as the result of Wood's anomaly,<sup>13</sup> which was firstly observed in diffraction gratings and occurs when a diffracted order becomes tangent to the plane of the grating. When the order disappears, the light intensity is redistributed among the remaining orders. Wood's anomaly takes place at the wavelength of

$$\lambda_{\text{wood}} = \frac{a_0}{\sqrt{i^2 + j^2}} \sqrt{\epsilon_d} \quad (4)$$

It is obvious that Wood's anomaly is related to the period of the hole array ( $a_0$ ) and the permittivity of the dielectric layer ( $\epsilon_d$ ).

### 3. THE NUMERICAL CALCULATIONS

By applying the full-vectorial three-dimensional (3D) finite-difference time-domain (FDTD) method,<sup>14</sup> we can calculate the transmission spectra of electromagnetic waves through the free-standing silver film with subwavelength holes in different geometries. During the calculation, the frequency-dependent permittivity of silver is based on the Lorentz-Drude model,<sup>15</sup> and the grid spacing is carefully chosen to guarantee convergence. For simplicity, the thickness of the Ag film is chosen as 320 nm and the diameter of the hole is 280 nm in the following calculations.

First we consider an infinite two-dimensional hole array schematically shown in Figure 1(a), where the period of the square array  $a_0$  is 750 nm. When the light illuminates the hole array normally, the transmission spectrum is illustrated in Figure 1(b). Three major transmission peaks are observed in the wavelength regime we have calculated. According to Eqs. (1)–(3), we can index the peaks as  $(1, 0)$  at 808 nm,  $(1, 1)$  at 601 nm, and  $(2, 0)$  at 530 nm,

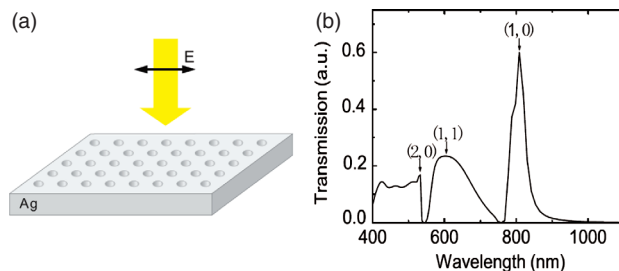


**Fig. 1.** (a) The schematic configuration for a silver film with two-dimensional hole arrays illuminated by light. (b) The calculated optical transmission spectrum of the structure at normal incidence. The major transmission peaks are indexed by two integers.

respectively, which are related to the SPs at the air-silver interface. And two transmission minima located obviously at the wavelength defined by Wood's anomaly. According to Eq. (4), when  $i^2 + j^2 = 1$  for the air-silver interface, the wavelength of the transmission minima is 750 nm; while for  $i^2 + j^2 = 2$ , the wavelength of minima is 530 nm.

In order to understand how the resonant modes appear in a subwavelength hole array, we calculate the transmission spectra and the electric field distribution of the hole system with different geometries (as shown in Figs. 2 and 3). Five different hole systems are included as following.

(1) An isolated hole perforated on silver film schematically shown in Figure 2(a), which we denote as "S1". When the light illuminates the sample "S1", a transmission peak appears at the wavelength of about 667 nm (as shown in Fig. 2(f)). Obviously, this peak is not predicted by Bethe's theory because surface modes are involved and evanescent modes can additionally be excited inside the hollow aperture. It has been shown that in the present system, the film plasmons induce a large dipole moment across the hole.<sup>16</sup> The hole thus mediates a coupling between these specific film plasmons and an incident electromagnetic wave, and this coupling depends on the hole size, the thickness of the film and the shape of the nanoholes. When the hole is ellipsoidal, both experiments and theory show that the plasmon mode that is polarized parallel to the short axis of the ellipsoidal hole red-shifts with increasing aspect ratio film.<sup>17</sup> Based on the distribution of electric field ( $E_z$ ) on the up surface of the film shown in Figure 3(a), it is found that the electric field becomes strong around the hole and it is evanescent till a few hundreds nanometer away from the hole. That is to say, LSPs are excited around the isolated hole, and contributes to the transmission.

(2) A square array of  $5 \times 5$  holes schematically shown in Figure 2(b), which we denote as "S2". The spacing between two neighbouring holes is 750 nm. It is obvious that even though the total number of the holes is very limited, three main transmission peaks of the structure have already been observed (as shown in Fig. 2(g)). These three peaks can be indexed as  $(1, 0)$ ,  $(1, 1)$ , and  $(2, 0)$ , respectively. Compare with the case of an infinite hole array (Fig. 1(b)), the transmission peaks in Figure 2(g)

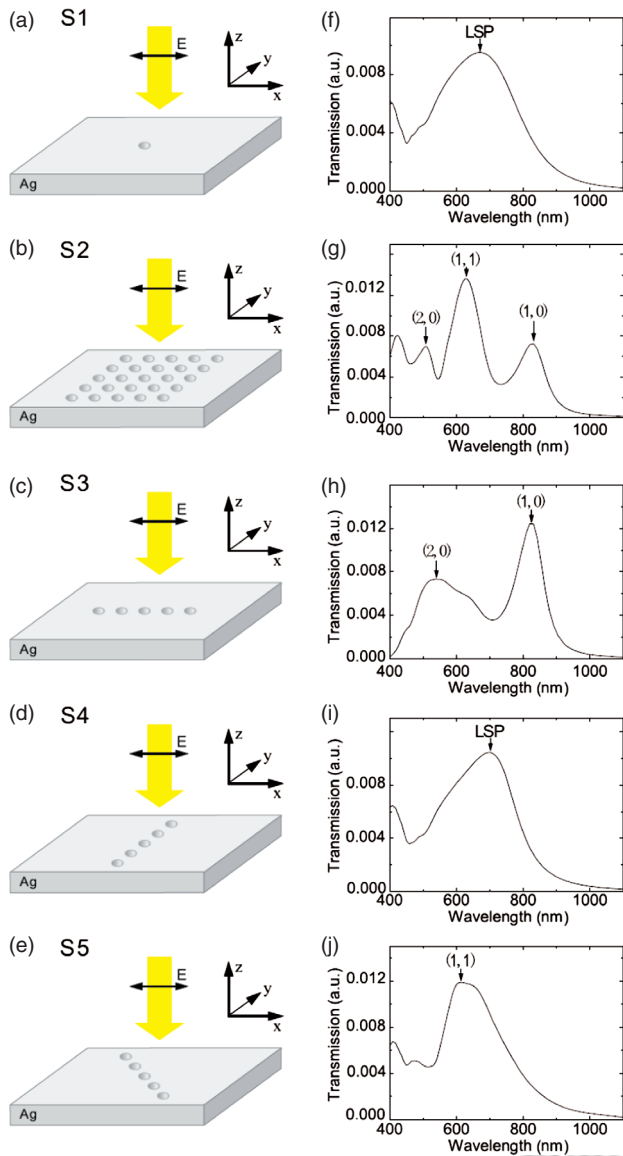


**Fig. 2.** The schematic silver films with the following aperture system illuminated by light and their calculated transmission spectra. In each case, the thickness of the Ag film is chosen as 320 nm and the diameter of the hole is 280 nm. (a) and (f): a single isolated hole perforated on silver film, which is denoted as “S1”. (b) and (g): a square array of  $5 \times 5$  holes spacing 750 nm, which is denoted as “S2”. (c) and (h): a 5-hole chain denoted as “S3”, which is parallel to the electric field of the incident light. (d) and (i): a 5-hole chain denoted as “S4”, which is perpendicular to the electric field of the incident light. (e) and (j): a 5-hole chain denoted as “S5”, where the angle between the chain and the electric field of the incident light is 45 degree.

have a little bit shift, which can be interpreted as effect of finite size.<sup>18,19</sup> The electric field distribution for the mode indexed by (1,0) has been calculated as shown in Figure 3(b). It is found that the localized electric field ( $E_z$ ) is strong around each hole, that is to say, LSPs are excited. Furthermore, the surface plasmons that propagate along  $x$  direction is obviously observed. Actually, strong electric fields ( $E_z$ ) distribute not only around the holes but in the

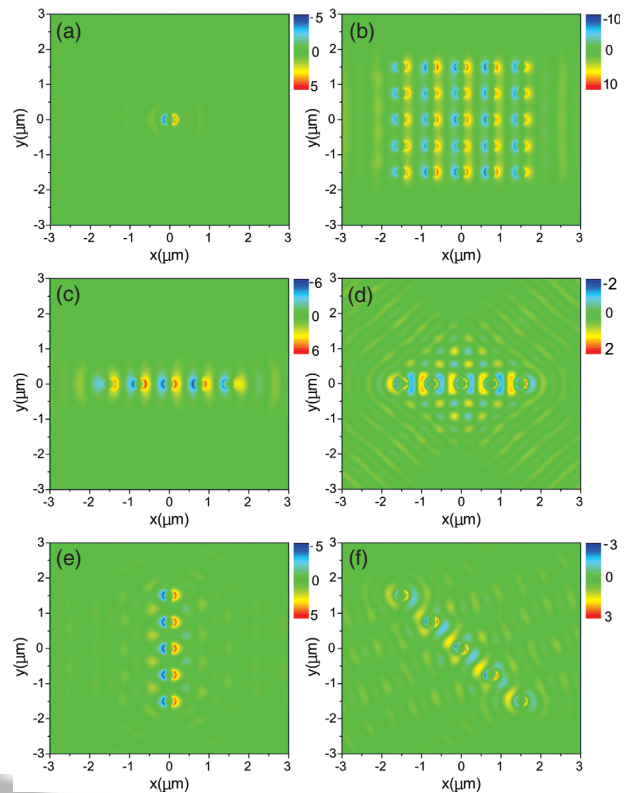


**Fig. 3.** The electrical field distribution ( $E_z$ ) of the resonant mode ( $\lambda_R$ ) on the up surface of the silver film with holes of different geometries. (a)  $\lambda_R = 667$  nm in S1. (b)  $\lambda_R = 830$  nm in S2. (c)  $\lambda_R = 820$  nm in S3. (d)  $\lambda_R = 540$  nm in S3. (e)  $\lambda_R = 698$  nm in S4. (f)  $\lambda_R = 613$  nm in S5.

whole film. Therefore, both LSPs and PSPs contribute to the transmission in this case.

(3) A 5-hole chain denoted as “S3”, which is parallel to the electric field of the incident light (as shown in Fig. 2(c)). In this case, two transmission peaks are observed (as shown in Fig. 2(h)), and these two peaks can be indexed as (1,0) and (2,0). In the electric field distribution of the mode (1,0), there is one maximum within a period along  $x$  direction (as shown in Fig. 3(c)); while in the electric field distribution of the mode (2,0), there are two maxima within a periodic along  $x$  direction (as shown in Fig. 3(d)). Compared with the case of a single hole (Fig. 3(a)), the distribution of electric fields in S3 is broader (Fig. 3(c)), which originates from the excitation of PSPs along  $x$  direction. Besides, if we compare the transmission spectrum of an infinite hole array (Fig. 1(b)) and the transmission spectrum in S3 (Fig. 2(h)), we can find that the peak indexed by (2,0) in Figure 1(b) has a blue shift from 540 nm to 530 nm, which comes from Wood’s anomaly occurring at the wavelength of 530 nm. Due to Wood’s anomaly, this peak is truncated and becomes obscure in Figure 1(b), however, it becomes evident in Figure 2(h).

(4) A 5-hole chain denoted as “S4”, which is perpendicular to the electric field of the incident light (as shown in Fig. 2(d)). Interestingly, the transmission peak in S4 (as shown in Fig. 2(i)) is very similar to the transmission one

of a single hole (S1, as shown in Fig. 2(f)) except a slight red shift. At this mode, the electric field is localized and becomes strong around each hole (as shown in Fig. 3(e)). This feature is also similar to the case of S1. Therefore, LSPs are excited in S4, but no PSPs are generated in S4. And the enhancement of transmission originates from the LSPs. The redshift we mentioned above may come from the interaction between the LSPs at two adjacent holes.

(5) A 5-hole chain schematically shown in Figure 2(e), which we denote as “S5”. In this case, the angle between the hole chain and the electric field of the incident light is 45 degree, and the separation of the holes is  $750 \times \sqrt{2}$  nm. In this case, the hole array provides a compensation of momentum of  $2\sqrt{2}\pi/a_0$ . The transmission peak is indexed as (1, 1) as shown in Figure 2(j). It is observed that PSPs propagate along the chain (as shown in Fig. 3(f)). Because both LSPs and PSPs are excited in S5, the transmission peak becomes very strong.

Besides, it is useful to compare both S3 and S4 in this work with the reported work on one-dimensional arrays of narrow slit milled on metal.<sup>20</sup> In Ref. [20], when the electric field of the incident light is parallel to the slit, PSPs can be excited and then enhance the transmission; while the electric field of the incident light is perpendicular to the slit, PSPs can not be excited. The features are similar to our finding in both S3 and S4.

#### 4. SUMMARY

We have investigated the propagation of light through an isolated subwavelength hole, the hole chain and the hole array with different geometries, respectively. Based on three-dimensional full-vector FDTD method, the optical transmission and the electromagnetic field distribution have been obtained. It is shown that that when the light illuminates an isolated subwavelength hole, LSPs are excited and contribute to transmission of the hole; while the light illuminates the hole chain and array, both LSPs and PSPs are excited, and their contributions to the transmission of holes strongly depend on the geometry of the hole chain and array, and also on the polarization of incident light. These results may have potential applications on designing plasmonic structures and devices.

**Acknowledgments:** This work was supported by grants from the National Natural Science Foundation of China (Grant Nos. 10625417 and 50672035), the State Key Program for Basic Research from the Ministry of Science and Technology of China (Grant Nos. 2004CB619005 and 2006CB921804), and partly by the Ministry of Education of China (Grant No. NCET-05-0440).

#### References and Notes

1. T. W. Ebbesen, H. J. Lezec, H. F. Ghaemi, T. Thio, and P. A. Wolff, *Nature* **391**, 667 (1998).
2. L. Martín-Moreno, F. J. García-Vidal, H. J. Lezec, K. M. Pellerin, T. Thio, J. B. Pendry, and T. W. Ebbesen, *Phys. Rev. Lett* **86**, 1114 (2001).
3. Z. H. Tang, R. W. Peng, Z. Wang, X. Wu, Y. J. Bao, Q. J. Wang, Z. J. Zhang, W. H. Sun, and M. Wang, *Phys. Rev. B* **76**, 195405 (2007); F. Gao, D. Li, R. W. Peng, Q. Hu, K. Wei, Q. J. Wang, Y. Y. Zhu, and M. Wang, *Appl. Phys. Lett.* **95**, 011104 (2009).
4. C. Genet and T. W. Ebbesen, *Nature* **445**, 39 (2007).
5. H. Liu and P. Lalanne, *Nature* **452**, 728 (2008).
6. Y. J. Bao, R. W. Peng, D. J. Shu, M. Wang, X. Li, J. Shao, W. Lu, and N. B. Ming, *Phys. Rev. Lett.* **101**, 08740 (2008).
7. C. Obermüller and K. Karrai, *Appl. Phys. Lett.* **67**, 3408 (1995).
8. A. Degiron, H. J. Lezec, N. Yamamoto, and T. W. Ebbesen, *Opt. Commun.* **239**, 61 (2004).
9. L. Yin, V. K. Vlasov, A. Rydh, J. Pearson, U. Welp, S. H. Chang, S. K. Gray, G. C. Schatz, D. B. Brown, and C. W. Kimball, *Appl. Phys. Lett.* **85**, 467 (2004).
10. E. Popov, N. Bonod, M. Nevière, H. Rigneault, P. F. Lenne, and P. Chaumet, *Appl. Opt.* **44**, 2332 (2005).
11. H. Bethe, *Phys. Rev.* **66**, 163 (1944).
12. E. Ozbay, *Science* **311**, 189 (2006).
13. R. W. Wood, *Philos. Mag.* **4**, 396 (1902); R. W. Wood, *Phys. Rev.* **48**, 928 (1935).
14. A. Taflov, Computational Electrodynamics: The Finite-Difference Time-Domain Method, 2nd edn., Artech House INC, Norwood (2000).
15. A. D. Rakic, A. B. Djurisić, J. M. Elazar, and M. L. Majewski, *Appl. Opt.* **37**, 5271 (1998).
16. T. H. Park, N. Mirin, J. B. Lassiter, C. L. Nehl, N. J. Halas, and P. Nordlander, *ACS Nano*. **2**, 25 (2008).
17. B. Sepulveda, Y. Alaverdyan, J. Alegret, M. Kall, and P. Johansson, *Opt. Express*. **16**, 5609 (2008).
18. J. Bravo-Abad, F. J. Garcia-Vidal, and L. Martín-Moreno, *Phys. Rev. Lett.* **93**, 227401 (2004).
19. F. Miyamaru and M. Hangyo, *Appl. Phys. Lett.* **84**, 2742 (2004).
20. J. A. Porto, F. J. Garcia-Vidal, and J. B. Pendry, *Phys. Rev. Lett.* **83**, 2845 (1999).

Received: 4 September 2009. Accepted: 30 October 2009.